Energy Advances

ROYAL SOCIETY OF CHEMISTRY

PAPER

View Article Online
View Journal

Cite this: DOI: 10.1039/d5ya00305a

Separation of tellurium from various tellurides relevant for photovoltaics and from pre-product thin film solar cells for recycling by chemical vapor transport

Lucas H. Bemfert, [a] Julian Burkhart, [a] Moritz Maxeiner, [a] Ruben Maile,[a] Victoria S. Drescher [a] and Klaus Müller-Buschbaum *[ab]

Thin-film solar cells based on CdTe are a viable technology for renewable energy generation due to their low production cost and relatively easy manufacturing. However, the scarcity and toxicity of Te necessitates the recovery of this element from end-of-life solar cells. In addition to CdTe, these solar cells contain several other tellurides, including Cu_2Te, ZnTe and SnTe. In this study, chemical vapor transport (CVT), using sulfur as a transport agent (TA), was utilised as an energy-efficient and waste-minimal method to separate Te from all the aforementioned tellurides in both open and closed systems. While transport rates of Te were demonstrated to be low in a closed system for CdTe and ZnTe, CVT in an open system can accelerate the procedure strongly, reaching recovery rates of 56% h^{-1} and 47% h^{-1} for CdTe and ZnTe respectively. The Te recovery rate for SnTe was 32% h^{-1}, which was eighty times higher for the open system than in a closed system at moderate T = 425 °C. For Cu_2Te, the open system even enabled Te transport that was not possible in the closed system. The feasibility of the CVT for recycling was further demonstrated by the use of pre-product thin film solar cells. *In situ* experiments utilizing a transport balance comparing CVT of Te starting from elemental Te and from CdTe or ZnTe revealed that the redox reaction does not seriously slow down the process.

Received 20th October 2025,
Accepted 22nd February 2026

DOI: 10.1039/d5ya00305a

rsc.li/energy-advances

Introduction

Photovoltaic technology plays an important role in addressing the energy transition from fossil energies to renewables.[1] Thin film solar cells based on CdTe have several advantages over the classical silicon-based ones such as their production being lower in cost, energy and material demand, global warming potential and ozone depletion potential.[2,3] Efficiencies of single CdTe-solar cells reach up to 21.1% and strategies for improving performance are being researched intensively, such as increasing the photocurrent, expanding the lifetime of charge carriers or better contacting of the back contact.[4,5] The annual installation of photovoltaic systems is steadily increasing, resulting in an expected waste volume of about 4.5 Mt of Te and 7.5 Mt of Cd in 2058.[6] The element Te is of particular interest because of its scarcity and the small number of countries where it is mined.[7,8] Te is primarily produced as a by-product during the mining of copper, zinc and lead ores, which has a price reducing effect, but also results in a significant dependence on these primary metals for the price and availability of Te.[9] To guarantee a steady supply of Te while minimizing waste, there is a strong demand for cost effective methods to recover Te from various sources. State of the art recycling techniques for CdTe solar cell recycling require large amounts of chemicals like HNO_3, H_2SO_4 and H_2O_2 for leaching and consequently produce a lot of waste.[10,11] Vacuum distillation is a fast and easy process but requires high temperatures.[12,13] For the production of very pure Te (>99.99999%), methods like zone refining are needed.[14,15]

An innovative method for recovery of Te from CdTe utilizing chemical vapor transport (CVT) was recently patented and published.[16,17] The process has already been implemented for the recovery of Te from Sb_2Te_3 and Bi_2Te_3, where remarkably high transport rates of up to 151 mg h^{-1} of Te were reached.[18]

The principle of a CVT is shown in Fig. 1. A CVT reaction occurs when a solid compound (E) interacts with a gaseous counterpart, the transport agent (TA), at a designated location, known as the source. While the other elements (X) remain at the source, E and TA form a new gaseous molecule, the

[a] Institute of Inorganic and Analytical Chemistry, Justus-Liebig-University Giessen, Heinrich-Buff Ring 17, 35392 Giessen, Germany. E-mail: kmbac@uni-giessen.de; Web: https://www.uni-giessen.de/en/faculties/f08/departments/iaac/buschbaum/index?set_language=en
[b] Center for Materials Research (LAMA), Justus-Liebig-University Giessen, Heinrich-Buff Ring 16, 35392 Giessen, Germany

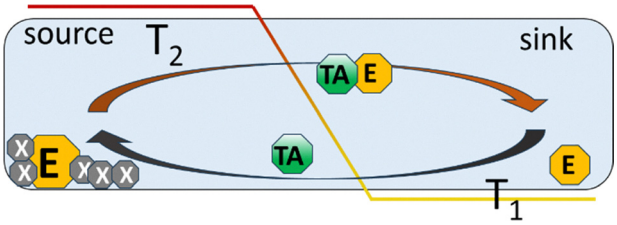

Fig. 1 The CVT concept: The transport agent (TA) reacts with an element or compound (E) at the source, forming the transport-active species (TA + E). This species then diffuses to the sink, where the backreaction occurs and E and TA are reformed, resulting in the purification of E.

so-called transport active species (TA + E). The solid is then reformed at a separate location, the sink, through changes in chemical equilibrium, typically achieved by altering temperature conditions. The higher temperature is designated as T_2, while the lower one is labeled as T_1. The temperature range between these points typically spans from 50 °C to 100 °C. The CVT can occur in either direction, from T_2 to T_1 or *vice versa* depending on the formation of the transport species being either endothermic or exothermic.[19]

A CVT for a chemical element requires a specific reactant as transport agent and a narrow temperature range in order to alter the chemical equilibrium. These defined conditions often result in the separation and purification of the element. This effect has been used commercially for a long time, for example in the Van Arkel-de Boer process.[20]

A method for recovering Sn by forming SnO for CVT has recently been published.[21] CVT using $AlCl_3$ and Cl_2 as TA was used for a recovery of rare earth elements (REE) as well as cobalt and nickel in an open flow tube, which was divided into 13 fractions with a temperature gradient from 1050 °C in the first fraction to 350 °C in the last fraction.[22] The first report on the CVT of Te with S as transport agent was published in 1976 by Binnewies.[23] A CVT of Te using I_2 as the transport agent was also demonstrated, requiring temperatures of 450 °C at the source and 350 °C at the sink, which are slightly higher than the temperatures used for the CVT with S.[24] The formation of H_2Te has also been observed and utilised for purification of Te, and for the preparation of Te single crystals.[25,26] Besides CdTe, other tellurides play an important role in modern CdTe thin-film solar cells. Doping CdTe with Cu results in good ohmic contact and higher hole concentration.[27] A high mobility of Te in Cu without the formation of Cu_xTe has been demonstrated by X-ray photoelectron spectroscopy (XPS) and photoluminescence (PL).[28] ZnTe is used as a buffer layer between CdTe and the contact material, which improves the module stability and reduces the thickness of the absorber layer.[29,30] The addition of SnTe improved open circuit voltage (V_{OC}) and acted as a barrier for minority carriers to enter the back contact.[31] SnTe is also used as a detector material in photodiodes.[32]

A variety of tellurides can be transported *via* the gas phase in processes in which the metal forms a transport active species, and the Te simultaneously sublimes. Solid solutions of CdTe with CdS as well as CdTe with CdSe and pure CdTe were transported with I_2 from 900 °C to 800 °C.[33,34] NH_4Cl was also used for a CVT of CdTe.[34] A CVT of ZnTe was performed with I_2 from 725 °C at the source to 623 °C at the sink.[35] ZnTe can also be transported with HCl as a TA, with 725 °C at the source and 650 °C at the sink.[36] I_2 was used to transport solid solutions of ZnTe and ZnS from 1000 °C at the source to 900 °C at the sink.[37] Also single crystals of SnTe were prepared by CVT from 800 °C to 750 °C with I_2 as the TA, as well as Sb-doped crystals by increasing both temperatures by 100 °C.[38] A CVT with I_2 was also possible for both SnTe and PbTe from 800 °C at the source and 700 °C at the sink.[39] The ternary compound $CuInTe_2$ was transported with I_2 in a temperature gradient from 650 °C to 600 °C.[40] However, a method of separating only Te from these tellurides using CVT is yet missing. As all these materials are relevant to the fabrication of CdTe thin film solar cells, they have now been investigated using S as the TA. Not only are the temperatures required lower compared to the CVT with I_2, but also exclusion of O_2 and H_2O is not as critical. In addition, the reaction of the chemicals contained in the pre-product thin-film solar cells and their effect on the separation of Te were tested.

Results and discussion

In a previously published process, the separation of Te from CdTe was demonstrated to be possible in both a closed and an open system by a CVT with S as TA.[17] In the closed system, a recovery of nearly 100% of Te in 72 h was possible with a T_2 = 400 °C. In the open-flow system, a temperature of T_2 = 425 °C enabled 20% of the Te to be recovered within 4 h. This is notably lower than the evaporation temperature of Te, which is 990 °C, and thereby ensuring energy savings and cost-effectiveness.[17]

The objective of this work was to apply this method to other relevant tellurides present in a CdTe thin-film solar cell, namely ZnTe, SnTe and Cu_2Te including real production material of solar cells. The primary questions addressed were: whether Te can be transported from these material components; if separation can be achieved, and if these additional components of a thin-film CdTe solar cell degrade the purity of the transported Te and the overall performance of the CVT. For a potential industrial application, genuinely pre-product thin film solar cells were included in the study, focusing on their separation and competition for CVT with S as a transport agent.

A particular emphasis was given to the yield of Te and the amount of Te that is transported per time, also known as the transport rate. Additionally, the purity of the transported Te was examined, along with the chemical composition of the material that did not undergo transportation. The CVT is described by the eqn (1) and (2) where either one or two Te atoms are incorporated into a sulfur ring, forming a gaseous mixed chalcogenide ring molecule. After diffusion to the sink, the change in temperature induces the back reaction to elemental Te and S. The latter remains in the gas phase and initiates the process anew after diffusion to the source.[23]

$$Te_{(s)} + S_{m,(g)} \rightleftharpoons TeS_{m,(g)} \qquad m = 1, \ldots, 7 \qquad (1)$$

$$2\,Te_{(s)} + S_{m,(g)} \rightleftharpoons Te_2S_{m,(g)} \qquad m = 1, \ldots, 6 \qquad (2)$$

Scheme 1 The reaction of Te with S forms mixed chalcogenide rings that function as transport-active species in the CVT.

$$XTe_{(s)} + 0.125\,S_{8,(l)} \longrightarrow XS_{(s)} + Te_{(s)} (\mathrm{X = Cd, Zn, Sn}) \qquad (3)$$

$$Cu_2Te_{(s)} + 0.125\,S_{8,(l)} \longrightarrow Cu_2S_{(s)} + Te_{(s)} \qquad (4)$$

$$2\,SnTe_{(s)} + 0.375\,S_{8,(l)} \longrightarrow Sn_2S_{3,(s)} + 2\,Te_{(s)} \qquad (5)$$

$$3\,SnTe_{(s)} + 0.5\,S_{8,(l)} \longrightarrow Sn_3S_{4,(s)} + 3\,Te_{(s)} \qquad (6)$$

$$SnTe_{(s)} + 0.25\,S_{8,(l)} \longrightarrow SnS_{2,(s)} + Te_{(s)} \qquad (7)$$

Scheme 2 Redox reactions for the formation of the elemental Te from the different tellurides (CdTe, ZnTe, SnTe and Cu_2Te) by reactions with S.

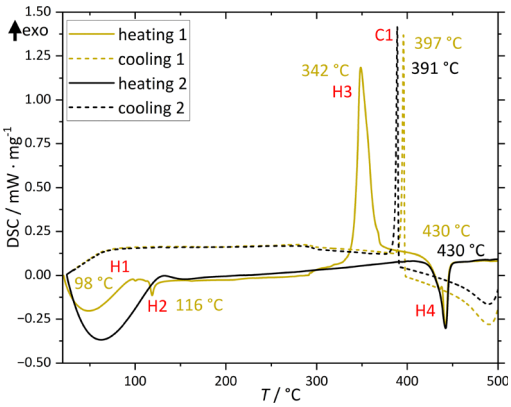

Fig. 2 DSC of a mixture of ZnTe and S with a molar ratio of 1 : 2. The temperatures depicted are the onset values marking the start of the processes.

Prior to the initiation of the CVT, S oxidises the telluride, resulting in the formation of elemental Te and the corresponding metal sulfides according to eqn (3) and (4), see also Fig. S69 and S70. For the reaction of SnTe with S, an oxidation of the Sn(II) has also been observed, leading to the formation of Sn_2S_3, Sn_3S_4 and SnS_2, according to eqn (5)–(7). In the case of Cu_2Te, the Cu(I)- ion was also oxidised, resulting in non-stoichiometric copper sulfides, see also Fig. S72 (Schemes 1 and 2).

The purity of the transported Te was checked with powder X-ray diffractometry (PXRD), scanning electron microscopy (SEM) with energy-dispersive X-ray spectroscopy (EDX) and microwave plasma atomic emission spectroscopy (MP-AES). From the remaining products at the source, Cd can be recovered by first oxidising the sulfides at 900 °C in air to CdO and then reducing CdO with methane at 750 °C and sublimation of elemental Cd in an open system.[17] In this study, a mixture of different metal oxides was tested to assess their impact on Cd recovery and the potential for Cd to become contaminated with other metals during sublimation.

Reaction conditions for the formation of Te

The formation reactions of Te-containing sulfur rings, which are the transport active species, are endothermic reactions, that determine the direction of the transport from higher to lower temperatures. To ensure an efficient CVT of Te with S, a temperature between 375–400 °C at the source is sufficient.[17,18,23] To keep the recovery of Te a one step process and to minimise energy consumption, it is important that the redox reactions of all present tellurides are inside or below this temperature range. To this end, DSC as well as *in situ* PXRD measurements were carried out to determine the temperatures at which reactions between S and ZnTe, SnTe, Cu_2Te or CdTe, respectively, may occur, and to identify potential side reactions.

Specific thermal properties of the system ZnTe/S

The DSC of ZnTe + S (Fig. 2 and Table 1) shows the anticipated signals of sulfur, including a phase transition from rhombic to monoclinic (98 °C, H1, endothermic) and the melting point (116 °C, H2, endothermic). A large signal (342 °C, H3, exothermic) corresponds to the formation of ZnS and Te, as validated through PXRD analysis of the sample post-measurement (SI, Fig. S14). The other signals are indicative of the melting of Te and S (430 °C, H4, endothermic) and the solidification of Te and S (397 °C/391 °C, C1, exothermic) during the cooling process. The redox reaction of ZnTe and S took place at an even lower temperature, 342 °C, than that of CdTe and S, at 350 °C, as observed in our previous study.[17] This is well below the temperature required for CVT, which is 375 °C.

In situ temperature dependent PXRD analysis of a mixture of ZnTe and S detected the formation of ZnS at 370 °C (see SI, Fig. S70), which is slightly higher than the temperature determined by DSC, indicating time required for crystallisation.

Specific thermal properties of the system SnTe/S

The products of the reaction of SnTe with S depend on the ratio of telluride to sulfur. For the DSC investigation, this ratio was chosen to be 1 : 2 (Fig. 3a) and 1 : 4 (Fig. 3b). The signals are listed in Table 2. The elevated excess of S leads to complete oxidation not only of telluride but also of Sn(II) to Sn(IV), which is confirmed by PXRD (SI, Fig. S16). In contrast, a lower excess of S resulted in formation of SnS and Sn_2S_3 during the reaction (PXRD, SI, Fig. S15). A signal for melting of S (110 °C, 114 °C, 117 °C, H1, endothermic) is present in both (a) and (b). The polymerization of S is only visible in (b) (158 °C/159 °C, H2, endothermic). Furthermore, a series of signals (H3, 290 °C, H4, 350 °C, H5, 399 °C, all exothermic) emerge with onset temperatures between 290 °C and 400 °C. This is indicative to a sequential oxidation of Sn(II) and the oxidation of Te(-II) to elemental Te.

These signals did not appear in the second heating run of either investigation, indicating a complete reaction with no connection to phase transitions of tin or tin sulfides, which is consistent with the phase diagram.[41] A DSC investigation of pure SnTe (SI, Fig. S3) also showed no signals in the respective temperature range, suggesting that the three signals are related

Table 1 Signals of the DSC measurement of ZnTe with S

Signal	Onset T run 1/°C	Onset T run 2/°C	Event	T/°C literature
H1	98	—	Phase transition of S from rhombic to monoclinic	95.3[42]
H2	116	—	Melting of monoclinic S	119.6[42]
H3	342	—	Formation of ZnS and Te	—
H4	430	430	Melting of Te in S	—
C1	397	391	Solidification of Te + S	—

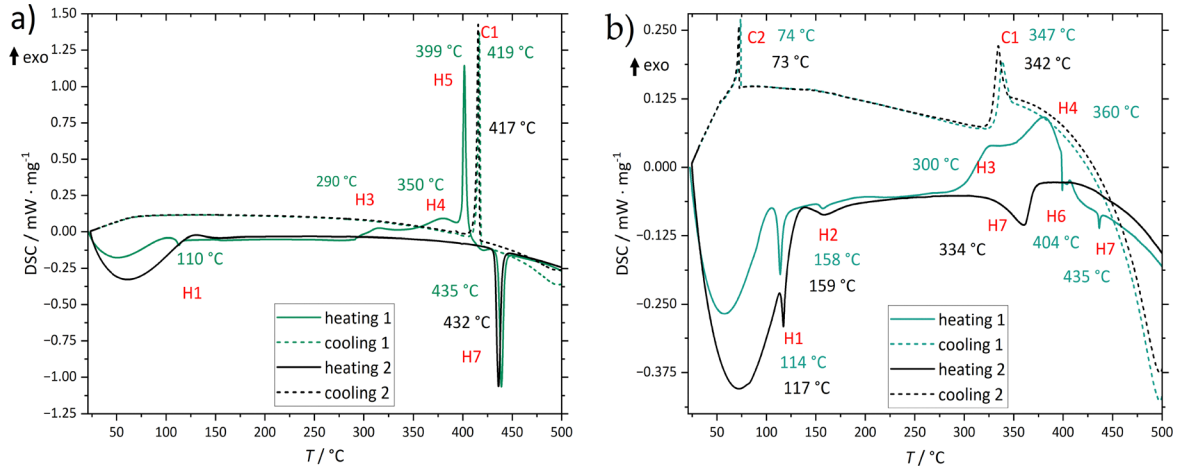

Fig. 3 (a) DSC of SnTe + S in a molar ratio of 1 : 2. (b) DSC of SnTe + S in a molar ratio of 1 : 4. The temperatures given are the onset values.

Table 2 Signals of the DSC measurements of SnTe with S

Signal	Onset T run 1 (a)/°C	Onset T run 2 (a)/°C	Onset T run 1 (b)/°C	Onset T run 2 (b)/°C	Event
H1	110	—	114	117	Melting of S
H2	—	—	158	159	Polymerisation of S
H3	290	—	300	—	
H4	350	—	360	—	
H5	399	—	—	—	
H6	—	—	404	—	Eutectic melting of 85% SnTe and 15% Te[43]
H7	435	432	435	334	Melting of Te in S
C1	419	417	347	342	Solidification of Te and S
C2	—	—	74	73	Solidification of S

to the redox reaction. *In situ* PXRD measurements of a SnTe + S mixture revealed reflections of SnTe as the only detectable Sn compound up to a temperature of 310 °C (SI, Fig. S71). At 350 °C, SnS_2 was the only detectable Sn species; no other tin sulfides could be observed. This suggests a one-step process at around 350 °C, which contrasts the DSC analysis findings showing three signals between 300 and 400 °C. This difference may be attributed the different experimental setups: a thin, densely packed glass capillary for the *in situ* PXRD analysis, and a quartz ampoule with some empty volume into which sulfur can evaporate and condense. The mixture in the glass capillary has a higher sulfur content to enable X-ray transmission, and the melting of sulfur may alter the local stoichiometry.

Additionally, two mixtures of 123 mg (0.5 mmol) SnTe and 64 mg (2 mmol) S were sealed in quartz ampoules and heated for 14 h to 300 °C and 350 °C respectively. PXRD investigations of both products revealed a high degree of similarity, showing only reflections for SnS_2 and Te (SI, Fig. S18). These findings indicate that both processes, oxidation of Te(-II) to Te(0) and of Sn(II) to Sn(IV), occur between 300 °C and 350 °C. A small signal in Fig. 3(b) (404 °C, H6, endothermic) may indicate melting of the eutectic mixture of 85% SnTe and 15% Te which is in accordance with the corresponding phase diagram.[44,45] Melting of Te and S (a) 425 °C/432 °C; (b) (435 °C/334 °C, H7, endothermic) occurs at higher temperatures, around 430 °C, and once at lower temperatures, 334 °C in the second run (b). Melting at the lower temperature occurs because the S content is higher, leading to a further lowering of the melting point of Te. The elevated melting point observed in the initial run can be attributed to most of the sulfur had been vaporised prior to the formation of Te during the redox reaction.

DSC analysis of mixtures of Cu_2Te and S was not informative, showing only melting points or no signals at all (SI, Fig. S4), because the mixture always already reacted immediately upon sealing the small DSC ampoule. However, *in situ* PXRD analysis of the mixture exhibited reflections for CuS at around 410 °C. After heating the mixture up to 450 °C and cooling down to room temperature, reflections were also found for Cu_2S, S and Te, see Fig. S72.

In situ PXRD analysis of a CdTe + S mixture (SI, Fig. S69) revealed CdTe reflections up to a temperature of 330 °C. At 350 °C, the main reflections were of CdS, with small reflections for CdTe also still visible. At higher temperatures, only reflections for CdS were observed, indicating that the redox reaction for the formation of CdS and Te occured at around 350 °C. This is consistent with the DSC results from our previous study.[17]

In summary, the exothermic signals observed in the DSC investigations, with onset temperatures ranging from 300 to 350 °C, combined with *in situ* PXRD results, suggest that the temperatures required for the redox reactions involving ZnTe and SnTe to produce elemental Te are similar to, or even lower than those previously observed for CdTe.[17] *In situ* PXRD revealed that the reaction of Cu_2Te with S required temperatures of around 410 °C. The oxidation of Sn(II) to Sn(III) or Sn(IV) resulting in the formation of Sn_2S_3 and SnS_2 requires a slightly higher input of S; however no undesirable side reactions were detected by DSC. The absence of other side reactions and the formation temperatures of Te remaining below 375 °C indicate that Te can be recovered from SnTe and ZnTe under conditions similar to those for the recovery of Te from CdTe.[17] This is favorable, as it allows for a recovery of tellurium from these phases in one step.

Transport reactions for the recovery of Te

The yield of an element for a CVT is calculated by dividing the mass m of the element that was transported to the sink by the total mass of the element in the system, which also equals the maximum amount that can be transported.

$$\text{Yield} = \frac{m_{\text{sink}}(\text{Te})}{m(\text{Te maximum})} \tag{8}$$

Dividing the yield by the duration the CVT was conducted leads to the recovery rate, which describes the effectiveness of the transport.

$$\text{Recovery rate } \dot{r} = \frac{\text{yield}}{t} \tag{9}$$

Another parameter for characterising a CVT is the so-called transport rate, $\dot{m}$, which quantifies the mass of a substance that is transported per unit of time. This signifies the efficiency with which the CVT operates, independent of the initial amount. This parameter can be calculated in two distinct ways: either after the CVT, according to eqn (10), or during the CVT, according to eqn (11). The first method involved dividing the mass of the product at the sink (m_{sink}) by the time for CVT (t).

$$\text{Transport rate } \dot{m} = \frac{m_{\text{sink}}(X)}{t} \tag{10}$$

When calculating the transport rate in this manner (eqn (10)), there are several factors that influence the reliability of the result. First, if the CVT is completed prior to the heating time of the oven, m_{sink} will no longer increase, thus t will be inadvertently extended, resulting in $\dot{m}$ being underestimated. This phenomenon is particularly pronounced when none of the transported elements remain at the source after CVT. Conversely, the presence of impurities, such as the transport agent which may deposit at the sink, can lead to an excessive m_{sink}, resulting in an overestimated $\dot{m}$.

An alternative approach to ascertain the transport rate involves the utilization of data obtained from a transport balance, which quantifies the mass of the transported product over time during the CVT in predetermined time intervals, typically of three minutes. Once the oven reaches the target temperature and the ampoule is in thermal equilibrium, the transport will be in a stationary state, resulting in a linear increase in m_{sink}, provided that no other side processes are occurring. The CVT continues until the product has been completely transported from source to sink. This results in a linear increase in m_{sink}, which can be described by eqn (11), enabling a calculation of $\dot{m}$ through linear regression. m_0 is the mass at the sink at the start of the CVT and is therefore assumed to be zero.

$$m_{\text{sink}}(t) = \dot{m} \cdot t + m_0 \tag{11}$$

A CVT can be configured as either a closed or open setup. The next section explains the distinct advantages and characteristics of each of the setups.

CVT of Te in a closed system with a transport balance

A CVT in a quartz ampoule describes a closed system, meaning no mass exchange with the outside and no substances can enter or leave the system. Therefore, the TA is continuously recycled during the back reaction, which reduces the required amount and keeps it constant throughout the CVT, different from an open system. This results in a steady state. However, the final pressure in the system should remain at approximately 1 bar, which limits the amount of TA that can be used. At this pressure, diffusion is the main mechanism for movement in the gas phase from source to sink and *vice versa*. Diffusion occurs considerably more slowly than the actual CVT reactions, thus acting as a limiting factor.[19] Two different setups were used to conduct the CVT in a closed system: the first involved using a transport balance to study the kinetics of the CVT. These experiments had several prerequisites. For example, the transported Te could be contaminated by the transport agent after the cooling. Therefore, a second set of CVT experiments was conducted in a closed system without using the transport balance to enable a higher sample throughput and higher Te purity. For experiments investigating the

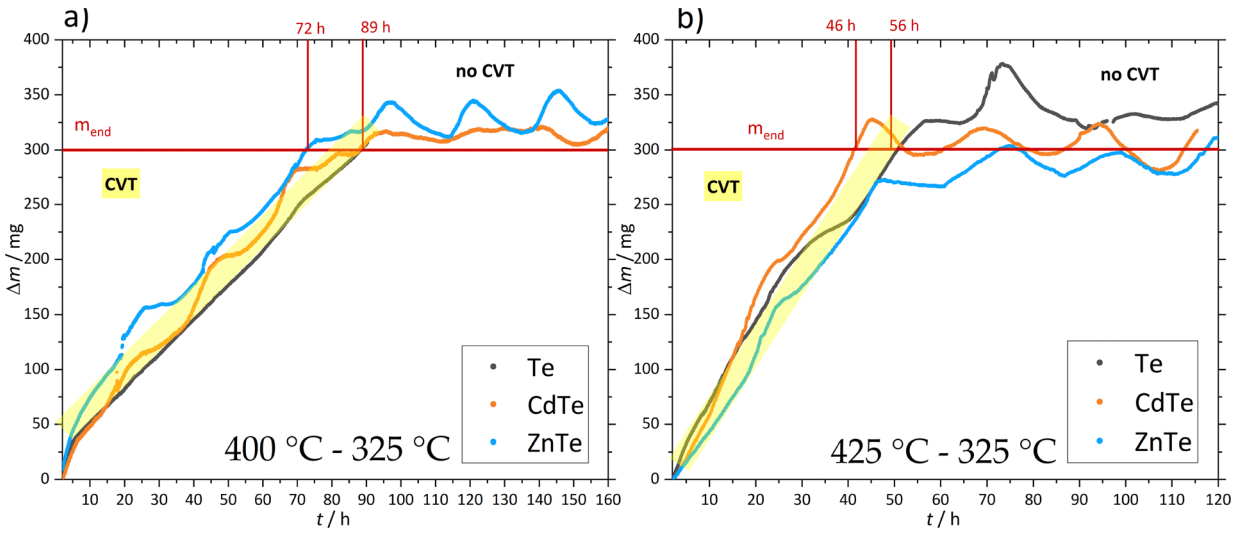

Fig. 4 Transported mass of tellurium from different tellurides over time by CVT with S from 400 °C to 325 °C (a) and 425 °C to 325 °C (b) starting from elemental Te, CdTe and ZnTe.

CVT of Te using the transport balance, two different temperature combinations were tested for three mixtures of educts: Te + S, CdTe + S, and ZnTe + S. The first temperature combination was T_2 = 400 °C and T_1 = 325 °C; the second was T_2 = 425 °C and T_1 = 325 °C. The results for the transported mass as a function of time are shown in Fig. 4 and a detailed list of all results can be found in Table S2 in the SI. For all tested tellurides, the measured mass on the scale increased linearly, indicating a steady state where the amount of transported Te is limited by the amount of TA. At around 300 mg the mass remained constant, which is the amount of Te in every sample and therefore the theoretical maximum increase for the mass. It should be noted that minor fluctuations in mass may be attributable to minor temperature variations within the laboratory environment. The linear increase in mass indicates that the CVT is taking place, while the constant mass and the 300 mg mass reached indicate the end of the transport reaction. This trend is consistent for all reactants at both temperatures, suggesting that the redox reaction for CdTe and ZnTe, leading to sulfide and Te formation, occurs rapidly and does not impede efficient transport. The transport rate of Te was determined for each experiment through two distinct methodologies. The initial approach involved a linear fit of the transport balance data for the time at which the CVT occurred (see eqn (11)). The secondary approach involved calculating the ratio of the product's mass at the sink to the CVT time (see eqn (10)). The resulting transport rates were found to be highly similar for both methods, thereby validating each other. However, an exception was observed for the ZnTe results with T_2 = 425 °C, where a slightly lower transport rate was observed. The transport rates were generally higher for elevated source temperatures. For instance, the rates at T_2 = 425 °C are 5.7 mg h^{-1}/5.9 mg h^{-1} for Te, 7.5 mg h^{-1} for CdTe and 6.8 mg h^{-1}/5.8 mg h^{-1} for ZnTe. The rates are all higher compared to the respective ones for T_2 = 400 °C (3.1 mg h^{-1}/3.2 mg h^{-1} for Te, 3.6 mg h^{-1} for CdTe and 3.7 mg h^{-1} for ZnTe). These results align with the expected behavior, as elevated temperatures result in increased diffusion, thereby promoting the transport.[17,18] As a result, the time for CVT was reduced from 72–90 h at 400 °C to only 46–56 h at 425 °C. The purity of the transported Te and the composition of the material at the source after CVT were examined using PXRD (SI, Fig. S22 and S23). Unlike the CVT experiments conducted without a transport balance, it was not possible to remove the ampoules from the oven during the cooling process, resulting in traces of S in Te at the sink. The presence of the sulfides CdS and ZnS was identified at the source as the products of CdTe and ZnTe, respectively (SI, Fig. S22 and S23). In the case of Te serving as the reactant, all of it was transported after the CVT, resulting in the absence of material at the source. This outcome is consistent with the findings of the DSC measurements, which have previously demonstrated that the redox reactions occur rapidly and at temperatures below those of the CVT. This observation also explains the similarity between the CVT experiments of CdTe and ZnTe in the closed system. For industrial applications, these findings indicate that the presence of various tellurides in the material does not significantly hinder the Te recovery. The similarity between the transport rates calculated by the two different methods supports the reliability of the results of the other CVT reactions in the following sections for both the closed and open system, for which more tellurides were tested. This is particularly important for the open system, where applying a transport balance is not possible. The transport rates are also within the same range, albeit slightly lower than those observed by Binnewies in 1976. Binnewies found rates of 7.5 mg h^{-1} for 20 mg S as TA and 6.1 mg h^{-1} for 10 mg S as TA at T_2 = 375 °C.[23] The CVT of Te with I_2 demonstrated a slightly higher transport rate of 19 mg h^{-1}, but required a higher T of 445 °C and a more complicated preparation.[24]

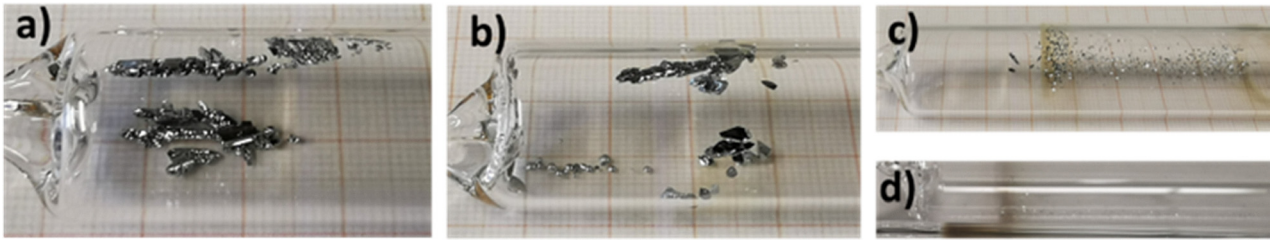

Fig. 5 Photographs of the transported product at the sink after CVT in ampoules from T_2 = 400 °C to T_1 = 325 °C for the different educts (a) CdTe. (b) ZnTe. (c) SnTe. (d) Cu_2Te.

CVT of Te in a closed system without a transport balance

Although the experiments using a transport balance were ideal for studying the kinetics of the CVT, they had several prerequisites. For instance, the transported Te could become contaminated by the transport agent during cooling. Therefore, a second set of CVT experiments was conducted in a closed system, enabling a higher sample throughput and higher Te purity, without using the transport balance. During the CVT, the transported product was deposited at the sink as intergrown crystals, as illustrated in Fig. 5, for CdTe (a) and ZnTe (b) as starting materials and as tiny flakes in the case of SnTe (c) and Cu_2Te (d). The products formed during a CVT of a duration of 72 h were analyzed using PXRD. For all reactions in the ampoules, the product formed at the sink was found to be Te, while the corresponding sulfides were formed at the source (SI, Fig. S6–S13). For the reactions involving Cu_2Te, SnTe and ZnTe at T_2 = 375 °C, the presence of elemental Te at the source was observed, indicating incomplete transport. The reactions with T_2 = 400 °C, starting with CdTe and ZnTe, showed no elemental Te at the source. For the reactions starting with SnTe, the formation of sulfides at the source was found to be dependent on the reaction temperature. At 375 °C, SnS_2 was formed, while SnS and S_2S_3 were detected after the reaction at 400 °C (SI, Fig. S10). The formation of copper sulfide through the reaction of Cu_2Te and S was incomplete, as evidenced by the continued presence of Cu_2Te at the source after the reaction (SI, Fig. S12). Additionally, elemental Te and various copper sulfides were detected at the source. MP-AES measurements were used to determine traces of the respective metals in the transported Te. Examination of all samples of the CVT with T_2 = 375 °C revealed that none of the respective metals were present above the limit of quantification (LOQ) of this method, which was 0.05 wt%, ensuring the transported Te to be of high purity (SI, Fig. S54 and S56). The transported amount of Te, the recovery rate, the yield, as well as the transport rate are listed in the SI (Table S1) for every telluride. The latter two are also presented in Fig. 6.

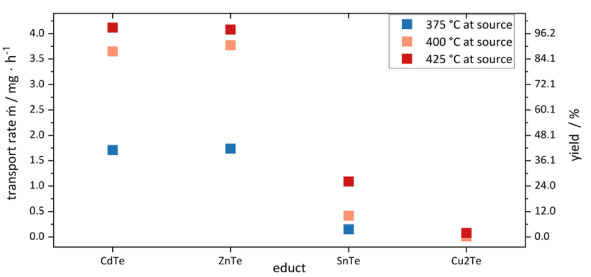

Fig. 6 transport rates of Te in the closed system for the different tellurides.

For all four tellurides, the transport rates for Te increased with increasing T_2. CdTe and ZnTe have the highest and similar values at every temperature, 1.7 mg h^{-1} at 375 °C, 3.7 mg h^{-1}/ 3.8 mg h^{-1} at 400 °C and 4.1 mg h^{-1} at 425 °C. At 425 °C, the yield approached 100%, indicating that the CVT was essentially complete before the conclusion of the experiment. This suggests that these transport rates are underestimating, which is supported by the results of the transport balance experiments, which gave Te transport rates of 7.5 mg h^{-1} for CdTe and around 6.2 mg h^{-1} for ZnTe as educt at 425 °C. A yield close to 100% also shows that almost all of the Te can be recovered using this CVT method. For SnTe, the Te transport rates are significantly lower with 0.2 mg h^{-1} at T_2 = 375 °C, 0.4 mg h^{-1} at T_2 = 400 °C and 0.8 mg h^{-1} at T_2 = 425 °C. This is due to the formation of SnS_2 and Sn_3S_4, which indicates the oxidation not only of the telluride, but also of Sn(II) to Sn(III) and Sn(IV). This consumes most of the sulfur, leaving very little for the CVT. A similar depletion of the TA occurs for Cu_2Te as starting material. This investigation showed almost no transported Te for T_2 = 375 °C, and diminutive transport rates of 0.01 mg h^{-1} for T_2 = 400 °C and 0.1 mg h^{-1} for T_2 = 425 °C, because Cu(I) was oxidised by S (SI Fig. S12). Following CVT, a yellow substance condensed at the walls of the quartz ampoules containing CdTe and ZnTe as the starting materials (SI Fig. S64 and S65). There was insufficient material of this substance for PXRD analysis, but SEM-EDX identified it as sulfur (SI, Fig. S73). Similar yellow deposits were found at the sink in CVT experiments in the open system, and could be additionally identified as sulfur by PXRD (SI, Fig. S68). The absence of sulfur in closed ampoule experiments containing SnTe and Cu_2Te confirms a depletion of S during the redox reaction (SI, Fig. S66 and S67), as does PXRD analysis of the source after the CVT. When SnTe is used as the starting material, Sn is only present in the sulfide compounds SnS, Sn_2S_3 and SnS_2 (SI, Fig. S10). As a result, the amount of sulfur in the source is accounting for more than 50% of the total amount. The same applies to Cu_2Te as starting material with twice as many Cu atoms as Te atoms, and CuS being found at the source after CVT (Si, Fig. S12). Thereby, more S is reduced

to form a sulfide than elemental Te is formed. In a closed system, the transport rates are generally quite low due to the limited amount of TA and the steady state of the CVT. Taking this into account, the Te transport rates are decent for CdTe and ZnTe and are comparable to other reports on CVT of Te.[17,18,23,24] However, for industrial applications, these rates are not particularly economical, and the rates for SnTe and Cu_2Te are negligible. Additionally, quartz ampoules are intended for single use only, resulting in high costs and waste production in a discontinuous process. Therefore, a CVT in a closed system is not a suitable setup for an intended application. Rather, it serves as a means of investigating the process under thermodynamic control. For industrial applications, a continuous process is significantly more favorable and can be achieved for a CVT in an open system with a flow tube, as outlined below.

CVT of Te from different tellurides in an open system

In the open system setup, the source and sink, with the temperatures T_2 and T_1 respectively, were connected by an open tube with an internal diameter of 14.5 mm and an inner cross-sectional area of 1.65 mm^2. A carrier gas (Ar) was passed through the tube at a constant flow rate of about 0.25 L h^{-1}. Consequently, there was a constant flow of volatile materials, resulting in a loss of the TA at the end of the tube. To mitigate this effect, the amount of TA was increased to 1.5 g of S at the source in these experiments. The telluride was mixed with S and placed in the first heating zone, acting as the source. The second heating zone acted as the sink with T_1 always at 325 °C. The last heating zone had a temperature of 200 °C and was used for condensation of the TA. For the second set of experiments, an additional amount of 1.5 g S was added into the system by evaporating it at 500 °C with a heating jacket and the quantity of telluride was doubled as well to keep the original ratio.

In the first set of experiments, the product that had been transported at the sink was distributed over a considerable length of approximately 20 cm, occurring in two shapes: crystal needles with lengths of a few millimetres, and small droplets or hemispheres. Both shapes were discernible to the naked eye (see Fig. 7a) and with the use of SEM (see Fig. 7b). For the following analysis, the products in the two shapes were mixed, ground in a mortar and analysed as one sample. The products formed at the sink were identified by PXRD as one phase: tellurium (SI, Fig. S7, S9, S11 and S13). Due to the time constraints of the CVT, oxidised but non-transported Te was also present at each individual source (SI, Fig. S6, S8, S10 and S12). This indicates that the transport of Te in the open system was not complete for the amount of S under the selected conditions. For CdTe and ZnTe, the redox reaction was found to be complete at both 400 °C and 425 °C, because no telluride was present at the source, and only sulfides were visible in the PXRD (SI, Fig. S6 and S8). SnTe reacted to SnS_2 at both temperatures, although some SnTe was still present after CVT at 400 °C (SI, Fig. S10). The redox reaction was also incomplete for Cu_2Te at both temperatures. In addition to Cu_2Te, elemental Te and Cu, as well as some copper sulfides were identified (SI, Fig. S12). The purity of the transported Te was verified through EDX measurements for the CVT with T_2 = 425 °C. For all the tellurides, the transported Te exhibited a purity of over 99.5 wt% Te, with trace amounts of sulfur (less than 0.3 wt%) present (SI, Fig. S57–S60). The samples were also analyzed by MP-AES, revealing that three out of four contained less than 0.05 wt% of the respective metal of the starting tellurides used for the reactions. For CdTe, a small amount of 0.1 wt% of Cd was identified in the transported Te (SI, Fig. S57).

The Te transport rates for the first setup in an open system were rather low, with a maximum of or about 10 mg h^{-1} being still comparable to the rates of the closed system (see SI, Fig. S1 and Table S3). It is possible that the S had left the system too quickly, resulting in a period of dead time during which no CVT occurred. In order to optimise the transport parameters and realise the potential of CVT in an open system, the CVT duration was reduced from four hours to one hour in the second set of experiments. Additionally, a further S 47 mmol (1.5 g) of S was introduced into the system *via* the gas phase, and the amount of telluride was increased accordingly to maintain the Te : S ratio. Fig. 8 presents the calculated Te transport rates and yields for the second open system setup.

The resulting transport rates for Te in the second setup were dramatically increasing to 142 mg h^{-1} for CdTe, 120 mg h^{-1} for ZnTe, 83 mg h^{-1} for SnTe and 29 mg h^{-1} for Cu_2Te. These transport rates are as high as those previously reported for Bi_2Te_3 (151 mg h^{-1}) and Sb_2Te_3 (121 mg h^{-1}) for which also an open setup was used.[18] Ultimately, CVT is no longer limited by a steady state when switching to an open system, which generally increases transport rates. Thus, the recovery rates increased to 56% h^{-1} for CdTe, 47% h^{-1} for ZnTe, 32% h^{-1} for

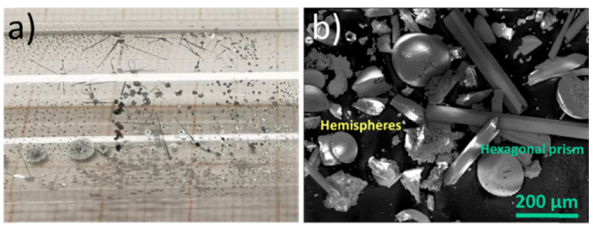

Fig. 7 (a) Photograph of the transported product at the sink. (b) SEM image of the transported product at the sink.

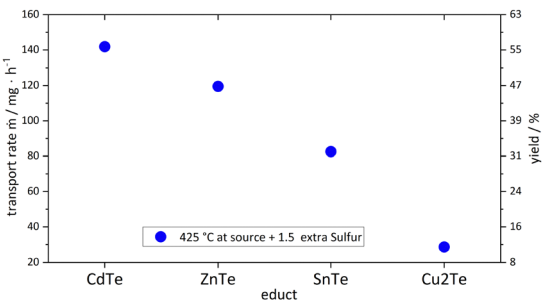

Fig. 8 Transport rates and yield of Te in the open system for the setup with a duration of 1 h and 1.5 g of additional S added after 30 minutes using a heating jacket.

SnTe and even 11% h^{-1} for Cu_2Te. For SnTe these values are even 80 times higher than for the closed system. For Cu_2Te, the rates in the open system setup were not just significantly higher than in the closed system experiments, but transport became feasible altogether, whereas almost no transport was observed in the closed system. In latter, only a small amount of TA is present, which must diffuse back to the sink in order to participate in the CVT again, being a time-consuming process. In contrast, in an open system, the amount of TA can be much higher, because it is not susceptible to overpressure resulting from evaporating the TA, as is the case in the closed system. Therefore, the amount of TA can be further adjusted by adding the TA in gaseous form. This was demonstrated in the second setup of experiments in the open system with S in an additional heating jacket before the transport tube. The enhancement in transport rates was particularly significant for SnTe and Cu_2Te, as the substantial excess of S compared to the closed system allows for a more thorough redox reaction to the respective sulfides and elemental Te.

PXRD investigations revealed the presence of Te at the source after the CVT for all the tellurides tested, as well as the presence of the respective metal sulfides (SI, Fig. S6, S8, S10 and S12). For SnTe as the starting material, only the compound SnS_2 was detected in addition to Te, indicating a complete oxidation of Sn(II) to Sn(IV). For Cu_2Te as starting material, Cu_2Te was also found at the source, showing again an incomplete reaction of Cu_2Te with S. No impurities of the transported Te at the sink could be detected using PXRD (SI, Fig. S7, S9, S11 and S13).

These experiments demonstrated that the CVT of Te from all the tested tellurides was possible in an open system, including SnTe and even Cu_2Te, ensuring a recovery of the Te from all relevant solar cell materials. It also demonstrates that CVT is much more feasible for recycling when used in an open system, particularly when additional S is added *via* the gas phase. Here, the transport time can be reduced in a way that up to 56% h^{-1} for CdTe, 47% h^{-1} for ZnTe, 32% h^{-1} for SnTe and even 11% h^{-1} for Cu_2Te could be transported. This means, in these experiments already more than of half of all Te from CdTe, the main telluride in thin-film solar cells, could be recovered within only 1 h.

Recovery of Cd

Once Te has been recovered by CVT, various metal sulfides remain at the source. These can be oxidised to their respective oxides at 900 °C open to air. After the reaction of the different metal oxides with CH_4, 111.8 mg of transported product were recovered and deposited as metallic mirrors on the walls of the tube. PXRD showed only the reflections of Cd (SI, Fig. S19) and EDX identified only the elements Cd and O (SI, Fig. S44 and S45). MP-AES revealed a high purity of the sublimed Cd, because the concentrations of Zn, Sn and Cu were below the limit of quantification, which was 0.05 wt% (SI, Fig. S61 and S62). Due to its low boiling point of 907 °C, Zn contamination was expectable, but did not occur.[46] At the source, 485.4 mg of material was recovered for which the phases ZnO, Sn, SnO_2 and CuZn could be identified by PXRD (SI, Fig. S20).

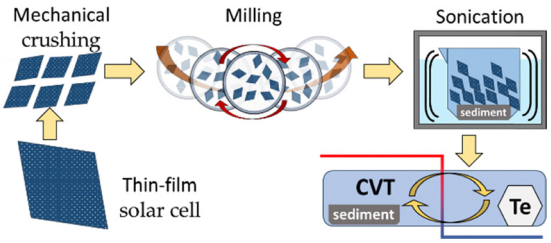

Fig. 9 Treatment of the solar cell samples for recovery of Te from mechanical crushing to the CVT reaction.

Recovery of Te from pre-product thin film solar cells

Having examined the potential for Te recovery through the reaction of tellurides with S and CVT with S, starting with a model system with pure chemicals, the next step was to conduct a final proof-of-principle experiment starting from real solar cell material. The pre-products of thin film solar cells and the sample treatment are outlined in Fig. 9. The used pre-product thin-film solar cells contained a glass plate with ITO, as well as the respective layers of CdTe, CdSe and ZnTe, and a metallic back contact. These plates were cut into smaller pieces, of which approximately 66 g were milled using a planetary ball mill. After the milling, only a small proportion of the shards were abraded but the major part of them was intact. Loose powder was found both at the bottom of the milling vial and stuck to the shards. The shards were cleaned by submerging them in isopropanol and ultrasonication for 30 minutes. After this, the shards had become transparent, indicating that the majority of the active layer had been removed. The shards were separated from the dispersion, after which the powder was collected by centrifugation and drying. This resulted in the recovery of 167 mg of powdered material, which primarily contained CdTe, as evidenced by PXRD (Fig. 10(a)). This material was mixed with 75.6 mg of S and subjected to CVT in an ampoule for 72 h with the heating conducted at T_2 = 400 °C and T_1 = 325 °C. A total of 8.5 mg of the product was recovered at the sink and a PXRD analysis (Fig. 10(b)) of the powder identified Te as the main phase. EDX (SI, Fig. S50) revealed a high Te content of >98 wt% and trace amounts of Se (0.7 wt%) as well as S (0.4 wt%), O and C. The C and O content can be explained

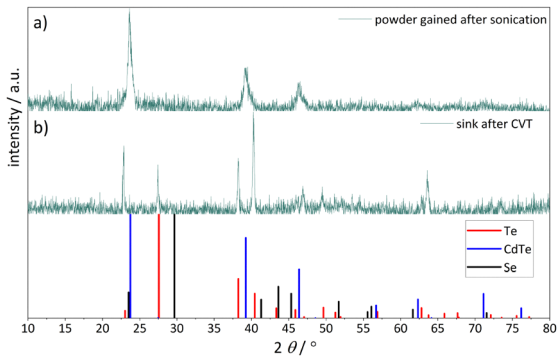

Fig. 10 PXRD of solar cell material after (a) sonication of glass shards, (b) sink of CVT of powder obtained after sonication.

by the carbon pad used for preparing the sample for SEM-EDX analysis.

The separation of Te from real solar cell material effectively illustrates the practical viability of the method on the first attempt. Therefore, these results serve as proof of concept for Te recovery by CVT with S as the TA. Another benefit is that the solar cells do not need to be completely crushed, because the powder adhering to the shards can be recovered through cleaning, as demonstrated in this study using sonication in isopropanol.

The purity of Te after a single transport process is also noteworthy, exceeding 98 wt%. The presence of Se in the transported Te is not unusual, because Se is volatile under the conditions used for this CVT.[47,48] Whether Te and Se can be separated *via* CVT remains to be researched. In addition, there are already established methods of separating Te and Se, including vacuum distillation and chemical treatments.[49–51]

Conclusion

This study successfully demonstrates the recovery of Te by reaction and subsequent CVT with S as transport agent (TA) being possible from all tellurides that were tested, namely CdTe, ZnTe, SnTe, and Cu_2Te, as well as from pre-product thin film solar cells. In the closed system, the Te transport rates for all tellurides were low, and nearly no CVT of Te occurred for Cu_2Te, due to the redox behavior involving the further oxidation of the Sn(II) and Cu(I), respectively, which depletes the TA. However, for CdTe and ZnTe, a yield of Te close to 100% was achieved at 425 °C demonstrating that it is possible to recover almost all of Te by CVT in a closed system.

In addition, Te transport rates could be dramatically increased for every telluride by conducting the CVT in an open system with S also added *via* the gas phase. An acceleration rate of the transport up to 80 times was achieved for SnTe and moreover, separation of Te from all tellurides was enabled, including Cu_2Te. Altogether, more than 50% of Te could be recovered with this CVT process in just one hour from the tellurides with the highest mass fraction in thin-film solar cells (CdTe and ZnTe).

In situ weighing utilizing a transport balance during the CVT indicated a linear increase in mass at the sink for Te, CdTe, and ZnTe as starting materials during CVT of Te. No significant differences were identified between CVT from tellurides compared to elemental Te. This suggests a rapid redox reaction between the tellurides and S, with minimal influence of the reaction time on the CVT of Te. For the telluride compounds investigated in this study, the oxidation of Te(-II) to elemental Te was achieved for CdTe and ZnTe. For SnTe and Cu_2Te, the oxidation was facilitated by increasing the amount of sulfur. Therefore, the oxidation of the telluride does not hinder Te recycling by CVT.

Furthermore, the simultaneous reduction and distillation of Cd from the metal oxides was successfully demonstrated, with no traces of other metals detected in the Cd deposited from the gas phase. This process enables the separation of the toxic element Cd from photovoltaic waste, preventing the release of toxic heavy metals and reducing the hazardousness of the residual electronic waste also in the presence of the other telluride phases present in a PV module.

Overall, oxidation of the tellurides CdTe, ZnTe, SnTe and Cu_2Te to elemental Te by S, followed by immediate CVT of Te with S, proved to be a suitable method for separating Te from all the tested tellurides and real solar cell materials. The purity of the transported Te was already quite high at 98% after a single transport. Especially, the processing of pre-product materials proofed the potential to recover a mixture of Te and Se from real thin film solar cell components, highlighting the feasibility of this process for recycling.

Altogether, the recycling method presented accomplishes several sustainability goals: It has a low energy demand due to the low temperatures required, it is considerably fast and uses low amounts of chemicals that can be recovered and re-used, further minimizing waste production. This could further encourage the use of CdTe thin-film technologies in addition to silicon-based photovoltaics despite critical and toxic elements and compounds involved in this technique.

Experimental

Transport reactions

Closed system. For the experiments in the closed system, the respective amounts of reagents and transport agent were placed in quartz ampoules (200 mm length, 14.5 mm diameter), followed by evacuation to ~0.001 mbar before fusing. The ampoules were then placed in an openable HMF tube oven from Horst GmbH with two independent heating zones controlled by HT MC 11 temperature controllers. A total of 93 mg (2.9 mmol) of S was weighed in along with 2.3 mmol of the respective telluride (561 mg CdTe, 451 mg ZnTe, 576 mg SnTe, 596 mg Cu_2Te). Following a complete redox reaction, 20 mg of S (0.6 mmol) are expected to remain as the transport agent for CVT.

Open system. Two different sets of experiments were tested for the open system. For both sets, a Carbolite TZF 12/65/550 oven featuring three independently controllable heating zones was used. Within this configuration, a quartz tube with an inner diameter of 14.5 mm was positioned. The reagents were placed in the first heating zone directly within the quartz tube (source), while the middle zone served as a sink for CVT. The last zone was designated for sulfur condensation. To ensure an inert atmosphere, an argon gas flow of 2 L h^{-1} was applied for 30 min before being reduced to 0.25 L h^{-1} at the start of heating. For the first set of experiments, a total of 47 mmol of S (1500 mg) were used for the transport agent, along with 1 mmol of the respective telluride (240 mg CdTe, 193 mg ZnTe, 246 mg SnTe, 254 mg Cu_2Te). For the second set of experiments, the quantity of telluride was increased to 2 mmol (480 mg CdTe, 386 mg ZnTe, 492 mg SnTe, 508 mg Cu_2Te). Additionally, a heating jacket (Horst HMT-900 °C) was placed around the quartz tube before the three-zone-oven. A further

47 mmol (1500 mg) of S was placed inside the tube at this spot. Therefore, the Te : S ratio remains the same for all investigated open system setups. The heating jacket was heated to 500 °C, 30 minutes after the three-zone-oven had reached the reaction temperature, to introduce more S as transport agent into the system. After 30 minutes, both ovens were switched off, resulting in a total duration of 1 h for the CVT.

Transport balance setup. A transport balance is a device used to track the progress of a CVT by determining the transported mass *in situ* using a lever mechanism. This concept was first described by Plies, Gruehn *et al.*[52] Over the years, the concept has been improved by several working groups and has enabled the determination of reaction enthalpies as well as entropies.[53,54] For instance, to determine the formation enthalpy of RhI_3, a configuration was constructed that incorporated a secondary oven, which was used to heat a reference ampoule at the opposing lever arm.[55] The device used in this study was built based on the models outlined in the reference publications. The configuration of the apparatus is illustrated in Scheme 3. In general, it consists of a seesaw with two corundum rods, oriented along the direction of the oven, where the ampoule is placed so that one end is in the centre of the first heating zone and the other end is in the centre of the second heating zone. The opposing end of one corundum rod extends beyond the oven and is supported by a programmable laboratory balance. This configuration enables the automated collection of measurement data in predetermined time intervals. The support for the force transition is composed of a tube with a metal spring inside and a plastic tip on top for vibration dampening. To mitigate vibrations originating from the building, the fulcrum and balance are placed on a granite plate that is covered by a box made of transparent polycarbonate and a frame of aluminium to shield the device from airflow. A movable metal block is clamped at the end of the corundum rod, enabling adjustment of the counterweight.

For the CVT experiments involving the transport balance, 300 mg (2.3 mmol) Te + 50 mg S (1.6 mmol), 561 mg (2.3 mmol) CdTe + 125 mg (3.9 mmol) S, and 450 mg (2.3 mmol) ZnTe + 125 mg (3.9 mmol) S were mixed, respectively, resulting in 50 mg (1.6 mmol) of S left as transport agent.

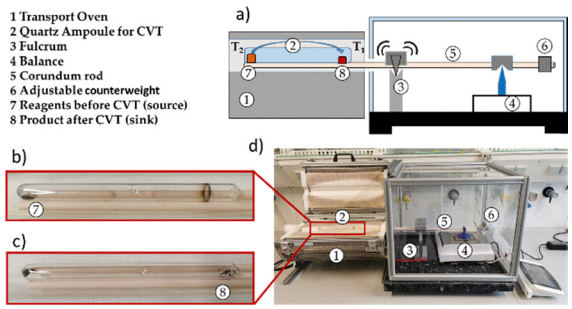

Scheme 3 (a) Depiction CVT setup with a transport balance. (b) Ampoule before CVT. (c) Ampoule after CVT with crystals at sink. (d) Photograph of the setup.

Separation of Cd from solar cell waste materials

The same setup that was used for the CVT in open systems was also utilised for the recovery of Cd from the reaction product of the tellurides, as well as from indium oxide (In_2O_3) subsequent to the first CVT. Prior to this, the remnants of the initial CVT at the source were oxidised at 900 °C for 14 h using air in a process demonstrated previously.[17] The experiments commenced with the oxides, resulting in a mixture of 257 mg (2 mmol) CdO, 162 mg (2 mmol) ZnO, 80 mg (1 mmol) CuO, 225 mg (1.5 mmol) SnO_2 and In_2O_3. This mixture was mortared and positioned in the first heating zone of the three-zone-oven within a quartz tube. The tube was then flushed with a flow rate of 4 L h^{-1} for 2 h. After this, the oven was heated up to 750 °C in the first zone, 650 °C at the second and 550 °C in the third heating zone. Once these temperatures had been reached, the Ar flow was terminated and replaced by 1.5 L h^{-1} of natural gas (92 mol% methane). After 2 h the sample cooled down by deactivating the furnace.

Preparation of powders from thin film solar cells for CVT

Samples of pre-product thin film solar cells were supplied by CTF Solar GmbH in the form of glass plates with a coating of the active layer (CdTe/CdSe), a buffer layer (ZnTe) and a metallic backcontact. The coated glass plates were broken down into small pieces measuring about 0.5 to 1 cm in diameter. Approximately 20 g of fragments were placed in a 25 mL stainless steel milling vial, and ground for 10 min at 350 rpm using a Retsch PM 200 planetary ball mill without adding any milling balls. The remaining glass fragments were washed by immersion in isopropanol and sonication for 30 min. The fragments were separated from the suspension, which was then centrifuged at 6000 rpm for 15 minutes using a Herolab UniCen MR. The resulting powder was used for CVT with S. 167 mg of powder was recovered by combining the products from three milling and sonication runs, with a total of 66.28 g of solar cell material being used as the starting material. The powder was mixed with 75 mg (2.3 mmol) S and heated to T_2 = 400 °C and T_1 = 325 °C for 72 h. The products were then analyzed by PXRD and SEM-EDX.

Powder X-ray diffractometry (PXRD)

X-ray powder diffraction patterns were obtained using an XPert Pro (PANalytical) instrument equipped with an Empyrean Cu LFF X-ray tube operating at 40 kV and 40 mA, along with an XCelerator detector. The incident beam path was equipped with a 0.04 rad Soller slit, a 10 mm beam mask, an anti-scatter slit of 1°, and a divergence slit of 1. Within the diffracted beam path, an anti-scatter slit of 0.5°, a 0.04 rad Soller slit, and a Nickel Beta-filter (0.02 mm) were positioned. The samples were placed on a sample holder with a silicon wafer and were flattened with a spatula. The diffraction pattern was recorded over the range of 10°–80° in 2Θ with a step size of 0.0167° by using monochromatic Cu-Kα radiation (λ = 150.46 pm).

In situ powder X-ray-diffractometry

In situ temperature dependent PXRD analyses were carried out using a Stoe Stadi P diffractometer (Darmstadt, Germany).

Equipped with a focusing Ge(111) monochromator and a Dectris Mythen 1K strip detector, in Debye–Scherrer geometry. The samples were prepared by grinding a 8 : 1 mass ratio mixture of sulfur and the respective tellurides (CdTe, ZnTe, SnTe and Cu_2Te) in a mortar. The powdered samples were filled in 0.3 mm glass capillaries (Hilgenberg Spezialglas Nr. 10), which were then sealed and placed in 0.5 mm diameter quartz capillaries (Hilgenberg quartz glass). All samples were measured in transmission geometry with Cu-K_α radiation (λ = 154.056 pm). The samples were heated up using the Stoe HT1 capillary furnace. Data collection was performed using the Stoe Powder Diffraction Software Package WinXPOW.

Thermal analysis

Differential scanning calorimetry. Differential scanning calorimetry (DSC) analysis was conducted on ZnTe, SnTe and the mixtures with S using a NETZSCH DSC-404-C instrument. The measurements were performed under an argon flow of 150 mL min^{-1} with a heating rate of 5 K min^{-1} in the temperature range of 20 °C to 500 °C, and two heating and cooling cycles were recorded for each sample. Quartz ampoules with specific dimensions (outer diameter: 6 mm; wall thickness: 1 mm; height: 10–15 mm) and a polished bottom were used for the measurements. The samples were carefully placed inside the ampoules, which were then securely attached to a quick-fit assembly. The assembly was evacuated to 0.001 mbar. During the sealing process of the ampoules, the sample-containing section was periodically cooled with liquid nitrogen, and cooled metal tweezers were used to handle it safely. A sample carrier equipped with a type E thermocouple was utilised for temperature measurement and sensitivity calibration. Standard materials, including indium (In), bismuth (Bi), lead (Pb), zinc (Zn), and aluminum (Al), had been used for calibration. The sample quantities used for the measurements were as follows: 15.7 mg of ZnTe (0.081 mmol) for pure ZnTe, 11.7 mg of SnTe (0.048 mmol) for pure SnTe and for the combined measurements 13.1 mg of a molar 1 : 2 ZnTe–S mixture, 13.4 mg for a 1 : 2 SnTe–S mixture and 14.5 mg for a 1 : 4 SnTe–S mixture.

SEM-EDX

Scanning electron microscopy (SEM) micrographs were obtained using a Gemini SEM 560 (Zeiss) system, operated at an acceleration voltage of 3 kV and a current of 100 pA with a working distance set to 5 mm. Energy dispersive X-ray spectral mappings were recorded utilizing an Ultim®MAX detector from Oxford Instruments. For these mappings, a working distance of 8.5 mm was applied, along with a current of 1 nA and an acceleration voltage of 8 kV. Prior to the imaging procedure, samples were carefully dripped onto sticky carbon pads affixed to the specimen holders. Any excess sample material was gently removed by applying pressurised air blown directly above the specimen holders. A 5 nm layer of platinum was sputtered onto the sulfur sample prior to measurement.

MP-AES

Microwave-assisted atomic emission spectroscopy (MP-AES) was used to determine the concentrations of impurities in the transported products with an MP-AES 4210 instrument from Agilent Technologies. Solutions of the samples with concentrations of 100 mg L^{-1} were prepared in HNO_3 ($c \sim 1\%$). The respective elements to be analyzed were added in different concentrations, ranging from 0.05 mg L^{-1} to 10 mg L^{-1} for a standard addition, to avoid an influence of the matrix on the measurement. Standard solutions (concentration of 1000 mg L^{-1}, Supelco®) of $Cd(NO_3)_2$, $Zn(NO_3)_2$, $Cu(NO_3)_2$ and $SnCl_4$ were purchased from Sigma Aldrich. The wavelengths considered were 228.802 and 326.106 for Cd, 213.857 nm and 481.053 nm for Zn, 303.412 nm and 317.505 nm for Sn and 324.754 nm and 327.395 nm for Cu.

Conflicts of interest

There are no conflicts to declare.

Data availability

The data supporting this article have been included as part of the supplementary information (SI). Supplementary information is available and contains detailed information on analytical results. See DOI: https://doi.org/10.1039/d5ya00305a.

Acknowledgements

The authors would like to express their sincere gratitude to Mrs Ivonne Bergen for conducting the MP-AES measurements. We would also like to thank CTF Solar GmbH for providing the CdTe thin film solar cell material. Additionally, we extend our appreciation to the Justus-Liebig University Giessen for providing startup financing for this work.

References

1 H. Lee, K. Calvin, D. Dasgupta, G. Krinner, A. Mukherji, P. W. Thorne, C. Trisos, J. Romero, P. Aldunce, K. Barrett, G. Blanco, W. W. Cheung, S. Connors, F. Denton, A. Diongue-Niang, D. Dodman, M. Garschagen, O. Geden, B. Hayward, C. Jones, F. Jotzo, T. Krug, R. Lasco, Y.-Y. Lee, V. Masson-Delmotte, M. Meinshausen, K. Mintenbeck, A. Mokssit, F. E. Otto, M. Pathak, A. Pirani, E. Poloczanska, H.-O. Pörtner, A. Revi, D. C. Roberts, J. Roy, A. C. Ruane, J. Skea, P. R. Shukla, R. Slade, A. Slangen, Y. Sokona, A. A. Sörensson, M. Tignor, D. van Vuuren, Y.-M. Wei, H. Winkler, P. Zhai, Z. Zommers, J.-C. Hourcade, F. X. Johnson, S. Pachauri, N. P. Simpson, C. Singh, A. Thomas, E. Totin, P. Arias, M. Bustamante, I. Elgizouli, G. Flato, M. Howden, C. Méndez-Vallejo, J. J. Pereira, R. Pichs-Madruga, S. K. Rose, Y. Saheb, R. Sánchez Rodríguez, D. Ürge-Vorsatz, C. Xiao, N. Yassaa, A. Alegría, K. Armour, B. Bednar-Friedl, K. Blok, G. Cissé, F. Dentener, S. Eriksen, E. Fischer, G. Garner, C. Guivarch, M. Haasnoot, G. Hansen, M. Hauser, E. Hawkins, T. Hermans, R. Kopp, N. Leprince-Ringuet, J. Lewis, D. Ley, C. Ludden, L. Niamir,

Z. Nicholls, S. Some, S. Szopa, B. Trewin, K.-I. van der Wijst, G. Winter, M. Witting, A. Birt, M. Ha, J. Kim, E. F. Haites, Y. Jung, R. Stavins, D. J. A. Orendain, L. Ignon, S. Park, Y. Park, A. Reisinger, D. Cammaramo, A. Fischlin, J. S. Fuglestvedt, J. R. Matthews and C. Péan, *IPCC, 2023: Climate Change 2023: Synthesis Report. Contribution of Working Groups I, II and III to the Sixth Assessment Report of the Intergovernmental Panel on Climate Change [Core Writing Team, H. Lee and J. Romero (eds.)]*, IPCC, Geneva, Switzerland, 2023.

2 E. Leccisi, M. Raugei and V. Fthenakis, The Energy and Environmental Performance of Ground-Mounted Photovoltaic Systems—A Timely Update, *Energies*, 2016, **9**, 622.

3 J. Peng, L. Lu and H. Yang, Review on life cycle assessment of energy payback and greenhouse gas emission of solar photovoltaic systems, *Renewable Sustainable Energy Rev.*, 2013, **19**, 255–274.

4 U. Manimaran and M. Shrinivas Dangate, A Review on Conducting Materials in CdTe Photovoltaic Cells, *ACS Omega*, 2025, **10**, 23858–23872.

5 A. Shah, A. P. Nicholson, T. A. M. Fiducia, A. Abbas, R. Pandey, J. Liu, C. Grovenor, J. M. Walls, W. S. Sampath and A. H. Munshi, Understanding the Copassivation Effect of Cl and Se for CdTe Grain Boundaries, *ACS Appl. Mater. Interfaces*, 2021, **13**, 35086–35096.

6 S. Mahmoudi, N. Huda and M. Behnia, Critical assessment of renewable energy waste generation in OECD countries: Decommissioned PV panels, *Resour., Conserv. Recycl.*, 2021, **164**, 105145.

7 R. Arvidsson, M. L. Söderman, B. A. Sandén, A. Nordelöf, H. André and A.-M. Tillman, A crustal scarcity indicator for long-term global elemental resource assessment in LCA, *Int. J. Life Cycle Assess.*, 2020, **25**, 1805–1817.

8 A. Urbina, Sustainability of photovoltaic technologies in future net-zero emissions scenarios, *Prog. Photovoltaics*, 2023, **31**, 1255–1269.

9 J. Jean, P. R. Brown, R. L. Jaffe, T. Buonassisi and V. Bulović, Pathways for solar photovoltaics, *Energy Environ. Sci.*, 2015, **8**, 1200–1219.

10 Z. Li, F. Qiu, Q. Tian, X. Yue and T. Zhang, Production and recovery of tellurium from metallurgical intermediates and electronic waste-A comprehensive review, *J. Cleaner Prod.*, 2022, **366**, 132796.

11 A. Mahmoudi, S. Shakibania, M. Mokmeli and F. Rashchi, Tellurium, from Copper Anode Slime to High Purity Product: A Review Paper, *Metall. Mater. Trans. B*, 2020, **51**, 2555–2575.

12 X. Zhang, D. Liu, W. Jiang, W. Xu, P. Deng, J. Deng and B. Yang, Application of multi-stage vacuum distillation for secondary resource recovery: potential recovery method of cadmium telluride photovoltaic waste, *J. Mater. Res. Technol.*, 2020, **9**, 6977–6986.

13 X. Yu, G. Zha, W. Jiang, B. Xu, D. Liu and B. Yang, Investigation of similar element selenium and tellurium volatilization behavior in the vacuum distillation separation process, *Vacuum*, 2025, **234**, 114098.

14 D. S. Prasad, N. R. Munirathnam, J. V. Rao and T. L. Prakash, Effect of multi-pass, zone length and translation rate on impurity segregation during zone refining of tellurium, *Mater. Lett.*, 2006, **60**, 1875–1879.

15 H. Chung, S. Friedrich, J. Becker and B. Friedrich, Purification principles and methodologies to produce high-purity tellurium, *CMQ*, 2024, **63**, 1626–1642.

16 G. Sextl, M. Binnewies, A. Bittner, K. Müller-Buschbaum, A. Sedykh, L. Bemfert, P. Schmidt and T. Donath, *Process and plant for obtaining tellurium*, WO/2023/117905.

17 L. H. Bemfert, J. Burkhart, A. E. Sedykh, S. Richter, E. L. Mitura, M. Maxeiner, G. Sextl and K. Müller-Buschbaum, Combinatorial Separation of Cd and Te from CdTe via Chemical Vapour Transport with Sulfur and Air/Methane Treatment for the Recovery of Critical Resources from Thin Film Solar Cells, *ChemSusChem*, 2024, e202400785.

18 J. Burkhart, L. Bemfert, E. Mitura, M. Maxeiner, R. Maile, A. E. Sedykh and K. Müller-Buschbaum, Tellurium Recovery from the Thermoelectric Materials Bismuth Telluride and Antimony Telluride by Chemical Vapour Transport, *Green Chem.*, 2025, **27**, 6405–6419.

19 M. Binnewies, M. Schmidt and P. Schmidt, Chemical Vapor Transport Reactions – Arguments for Choosing a Suitable Transport Agent, *Z. Anorg. Allg. Chem.*, 2017, **643**, 1295–1311.

20 A. E. van Arkel and J. H. de Boer, Darstellung von reinem Titanium-, Zirkonium-, Hafnium- und Thoriummetall, *Z. Anorg. Allg. Chem.*, 1925, **148**, 345–350.

21 Z. Su, W. Hou, J. Wang, Y. Zhang and T. Jiang, One-step separation of tin from e-waste by a chemical vapor transport process (CVT): Preparation of nano-SnO2, *Waste Manage.*, 2023, **157**, 330–338.

22 K. Murase, K.-I. Machida and G.-Y. Adachi, Recovery of rare metals from scrap of rare earth intermetallic material by chemical vapour transport, *J. Alloys Compd.*, 1995, **217**, 218–225.

23 M. Binnewies, Das Massenspektrum des Systems Te/S und der chemische Transport von Tellur mit Schwefel, *Z. Anorg. Allg. Chem.*, 1976, **422**, 43–46.

24 J. Burmeister, Crystal Growth of Tellurium by Chemical Transport, *Mater. Res. Bull.*, 1971, **6**, 219–223.

25 L. Mochalov, A. Logunov, A. Vorotyntsev, V. Vorotyntsev and A. Mashin, Purification of tellurium through thermal decomposition of plasma prepared tellurium hydride, *Sep. Purif. Technol.*, 2018, **204**, 276–280.

26 N. Chaudhary, A. Lakhani and D. Kumar, Open-ended chemical vapor transport method for growth of tellurium single crystals with tunable carrier concentration, *Mater. Today Chem.*, 2025, **46**, 102714.

27 M. Houshmand, M. H. Zandi and N. E. Gorji, SCAPS Modeling for Degradation of Ultrathin CdTe Films: Materials Interdiffusion, *JOM*, 2015, **67**, 2062–2070.

28 W. Xia, H. Lin, H. N. Wu, C. W. Tang, I. Irfan, C. Wang and Y. Gao, Te/Cu bi-layer: A low-resistance back contact buffer for thin film CdS/CdTe solar cells, *Sol. Energy Mater. Sol. Cells*, 2014, **128**, 411–420.

29 Daouda, F. Tchangnwa Nya, G. M. Dzifack Kenfack, A. Laref and A. Mohamadou, Multilayers strategy with a mixed CdTe/ZnTe absorber layer for optical trapping and efficiency improvement in CdTe-based solar – SCAPS modelling, *Phys. Scr.*, 2024, **99**, 055964.
30 C. A. Wolden, A. Abbas, J. Li, D. R. Diercks, D. M. Meysing, T. R. Ohno, J. D. Beach, T. M. Barnes and J. M. Walls, The roles of ZnTe buffer layers on CdTe solar cell performance, *Sol. Energy Mater. Sol. Cells*, 2016, **147**, 203–210.
31 Z. Weng, S. Ma, H. Zhu, Z. Ye, T. Shu, J. Zhou, X. Wu and H. Wu, CdTe thin film solar cells with a SnTe buffer layer in back contact, *Sol. Energy Mater. Sol. Cells*, 2018, **179**, 276–282.
32 V. Bodarya, H. S. Jagani, A. Patel, C. U. Vyas, J. Gohil and V. M. Pathak, Investigations of photo-transient properties and applications as photosensors in well-characterized tin telluride (SnTe) single crystal, *Mater. Chem. Phys.*, 2024, **314**, 128879.
33 U. Hotje and M. Binnewies, Chemischer Transport fester Lösungen. 20 [1] Der Chemische Transport von Mischphasen in den Systemen CdS/CdTe und CdSe/CdTe, *Z. Anorg. Allg. Chem.*, 2005, **631**, 1682–1687.
34 C. Paorici, V. Pessina and L. Zecchina, Interface Kinetical Limitations in Closed-Tube Chemical Vapour Transport (I), *Cryst. Res. Technol.*, 1986, **21**, 1149–1152.
35 H. Ogawa, N. Nishio and T. Arizumi, Epitaxial Growth and Chemical Vapor Transport of ZnTe by Closed-Tube method, *J. Cryst. Growth*, 1981, **52**, 263–268.
36 M. Nishio and H. Ogawa, Chemical vapor transport in the ZnTe-HCl Closed-Tube system and its thermodynamic analysis, *J. Cryst. Growth*, 1986, **78**, 218–226.
37 C. Rose and M. Binnewies, Chemischer Transport fester Lösungen. 12 [1] Der Chemische Transport von Mischphasen im System ZnS/ZnTe, *Z. Anorg. Allg. Chem.*, 2004, **630**, 1296–1300.
38 R. M. Kannaujiya, S. H. Chaki, A. J. Khimani, A. B. Hirpara, Z. R. Parekh, R. K. Giri, S. Patel and M. P. Deshpande, Effect of Sb doping on CVT grown SnTe single crystals electrical and thermal properties, *J. Mater. Sci.: Mater. Electron.*, 2022, **33**, 20823–20836.
39 O. Bosholm and H. Oppermann, Investigations of the Chemical Transport of Intermetallic Phases, I: GeTe, SnTe, PbTe, *Z. Naturforsch. B*, 1999, **54**, 737–746.
40 P. Prabukanthan and R. Dhanasekaran, Growth of CuInTe2 single crystals by iodine transport and their characterization, *Mater. Res. Bull.*, 2008, **43**, 1996–2004.
41 G. Lindwall, S. Shang, N. R. Kelly, T. Anderson and Z.-K. Liu, Thermodynamics of the S–Sn system: Implication for synthesis of earth abundant photovoltaic absorber materials, *Sol. Energy*, 2016, **125**, 314–323.
42 B. Meyer, Elemental sulfur, *Chem. Rev.*, 1976, **76**, 367–388.
43 A. S. Hakeem, S. M. AlMansour, M. A. Ehsan, Q. Drmosh, A. I. Bakare, F. Patel and S. Ali, Microstructural and thermal evaluation of the formation of tin–tellurium (Sn Te) alloy by ball milling process, *Powder Technol.*, 2023, **428**, 1–9.
44 R. C. Sharma and Y. A. Chang, The Sn-Te (Tin-Tellurium) system, *Bull. Alloy Phase Diagrams*, 1986, **7**, 72–80.
45 V. L. Kuznetsov, System Sn-Te: Critical Evaluation and Optimization of Data on the Thermodynamic Properties and Phase Diagram, *Neorg. Mater.*, 1996, **32**, 231–242.
46 Y. Zhang, J. R. G. Evans and S. Yang, Corrected Values for Boiling Points and Enthalpies of Vaporization of Elements in Handbooks, *J. Chem. Eng. Data*, 2011, **56**, 328–337.
47 Y. P. Kirillov, V. A. Shaposhnikov, L. A. Kuznetsov, V. S. Shiryaev and M. F. Churbanov, Modeling of the evaporation of liquids and condensation of their vapor during distillation, *Inorg. Mater.*, 2016, **52**, 1183–1188.
48 G. Zha, Y. Zhao, H. Luo, W. Jiang, B. Xu and B. Yang, Evaporation Regularities of Elemental Selenium in the Vacuum Distillation Process, *Metall. Mater. Trans. B*, 2022, **53**, 3856–3864.
49 H. Luo, W. Wang, X. Yu, X. Lei, L. Liu, G. Zha, W. Jiang, B. Yang and B. Xu, Novel valence regulation-vacuum gasification method for separation of selenium and tellurium, *Vacuum*, 2024, **219**, 112737.
50 J. E. Hoffmann, Recovering Selenium and Tellurium from Copper Refinery Slimes, *JOM*, 1989, **41**, 33–38.
51 H. Luo, W. Jiang, H. Xiong, G. Zha, L. Liu, T. Zhen, B. Yang and B. Xu, Selective Separation of Tellurium and Copper from Crude Selenium by Pre-oxidation and Vacuum Distillation, *Metall. Mater. Trans. B*, 2022, **53**, 1173–1182.
52 V. Plies, T. Kohlmann and R. Gruehn, Eine Methode zur kontinuierlichen Bestimmung von Transportraten Experimente im System GeO 2/WO 2/H 2 O und NiSO 4/PbSO 4/PbCl 2, *Z. Anorg. Allg. Chem.*, 1989, **568**, 62–72.
53 A. Hackert and V. Plies, Eine neue Methode zur Messung von temperaturabhängigen Partialdrücken in geschlossenen Systemen. Die Bestimmung der Bildungsenthalpie und -entropie von PtI2(s), *Z. Anorg. Allg. Chem.*, 1998, **624**, 74–80.
54 R. Heinemann and P. Schmidt, Crystal Growth by Chemical Vapor Transport: Process Screening by Complementary Modeling and Experiment, *Cryst. Growth Des.*, 2020, **20**, 5986–6000.
55 B. Commerscheidt and R. Gruehn, Die Bestimmung der Bildungsenthalpie von RhI3,s mit Hilfe einer weiterentwickelten Wägemethode zur Messung temperaturabhängiger Partialdrücke in geschlossenen Systemen, *Z. Anorg. Allg. Chem.*, 2001, **627**, 465–471.